sustainability

MDPI

Article

Fresnel Lens Solar Pumping for Uniform and Stable Emission of Six Sustainable Laser Beams under Non-Continuous Solar Tracking

Cláudia R. Vistas, Dawei Liang *, Miguel Catela, Hugo Costa, Dário Garcia, Bruno D. Tibúrcio and Joana Almeida

Centro de Física e Investigação Tecnológica (CEFITEC), Departamento de Física, Faculdade de Ciências e Tecnologia, Universidade NOVA de Lisboa, 2829-516 Caparica, Portugal
* Correspondence: dl@fct.unl.pt

Abstract: A multirod solar laser approach is here proposed to attain uniform and stable multibeam emission under non-continuous solar tracking. A Fresnel lens was used as the primary concentrator. The laser head was composed of a second-stage aspherical lens with a light-guide homogenizer and a third-stage conical pump cavity with six Nd:YAG rods. The solar laser system was optimized through numerical analysis in both Zemax® and LASCAD™ software to obtain six 1064 nm laser beams of similar multimode power. To investigate the effect of the homogenizer on the laser performance, the laser head was compared with a similar one that only used the aspherical lens in the second stage. The approach with the light guide attained a slightly lower efficiency than the one without the light guide; however, the tracking error width at 10% laser power loss was higher and, most importantly, only a 2.17% coefficient of variation of the laser power emitted by the six rods at the tracking error angle of $\pm 0.5^{\circ}$ was obtained. This is 4.2 times better than the 52.31% obtained with the laser head without the homogenizer and 76 times better than that of the previous numerical work. The light guide is thus essential to ensure uniform and stable solar laser power extraction from all rods even under non-continuous solar tracking, making this prototype the ideal for multibeam laser applications where uniformity and stability of the laser power are indispensable. This renewable multibeam solar laser may replace the classical lamp- and diode-pumped lasers, therefore ensuring a sustainable laser power production pattern for both space and terrestrial applications.

Keywords: Fresnel lens; solar laser; energy harvesting; stable emission; uniformity; tracking error; sustainable laser beam

Citation: Vistas, C.R.; Liang, D.; Catela, M.; Costa, H.; Garcia, D.; Tibúrcio, B.D.; Almeida, J. Fresnel Lens Solar Pumping for Uniform and Stable Emission of Six Sustainable Laser Beams under Non-Continuous Solar Tracking. *Sustainability* **2023**, *15*, 8218. https://doi.org/10.3390/su15108218

Academic Editor: Sebastiano Vasi

Received: 12 April 2023
Revised: 5 May 2023
Accepted: 15 May 2023
Published: 18 May 2023

1. Introduction

Renewable energy has a growing interest due to the current global energy crisis. Solar energy is one of the most explorable and vast energy sources used in different applications from photovoltaics (PV) to laser pumping, producing narrowband, collimated, and renewable laser radiation [1,2].

Renewable solar lasers rely on a nearly eternal and sustainable source, suppressing the need for expensive electrical pumping sources and their conditioning equipment. Their simplicity and reliability bring new opportunities to various laser-based applications, such as renewable energy cycles and materials processing, in off-grid locations [3], providing an important economic advantage for countries with high solar availability and for the future development of sustainable industrialization. The solar laser also offers ground-breaking solutions to space applications, such as free-space optical communications, space-to-Earth wireless power transmission, and photovoltaic energy conversion [4–6]. Although well-known materials such as Si and GaAs have achieved record efficiencies for single-junction PV cells under full spectrum illumination, it is important to consider that other materials may be more suitable for achieving high efficiency under monochromatic illumination [7].

The direct conversion of free broadband sunlight into laser light radically simplifies the complex electrically powered diode laser pumping solutions in space. The potential breakthroughs of solar lasers for space applications may be characterized by: (a) an improved reliability and lifetime, (b) increased overall efficiency, (c) reduced laser system complexity, (d) retrenchment on a system level (power supply, heat removal, redundancy), and (e) enabling novel space laser applications. In terms of the cost and maintenance, the solar laser has clear advantages over PV cell + diode-pumped or lamp-pumped laser approaches in space. Since the pump source is the Sun, shining nearly eternally in space, solar laser systems require little to no maintenance in terms of the pump source, making them an attractive option for long-lifetime space missions [8].

Primary concentrators are usually part of the first stage to concentrate the solar power to excite the laser medium. Among the main factors that influence the choice of concentrator are the efficiency, accessibility, cost, and ease of manufacturing. Parabolic mirrors benefit from the high solar flux attained. However, they are expensive, heavy, and not easily available. On the contrary, Fresnel lenses are low cost, lightweight, and easy to produce. Their drawback is their chromatic aberration, which decreases their efficiency. Nevertheless, unlike the parabolic mirrors, the laser head is positioned behind the Fresnel lenses and thus no shadows are created. Both primary concentrators have been used for solar laser research [3,9–15]. Using a parabolic mirror, the record solar laser collection efficiency and solar-to-laser conversion efficiency with a single laser rod are 38.2 W/m^2 and 4.5%, respectively [14].

All the above-mentioned achievements were based on the single-laser/single-beam concept. However, the utilization of multiple laser beams has been rapidly growing in laser research [16,17]. The implementation of a multibeam system within a compact laser head has been shown to be a highly effective method to reduce the processing time, quickly performing tasks where a single beam would need days or even weeks [18]. In solar laser technology, multiple beams can be extracted from a single laser head that has several laser rods [19]. In this way, the pump rays that are not completely absorbed by one rod can be further absorbed by others, ensuring an efficient absorption of solar pump energy. Moreover, the application of multiple thin rods in a single pump cavity leads to a distribution of the highly concentrated solar radiation among the rods, which alleviates the thermal stress, thermal lensing, and thermal fracture issues, enabling a better laser power scalability. The limitation to the maximum number of laser rods is based on the idea of avoiding superfluous system complexity and cost. In 2020, successful simultaneous emission of three 1064-nm solar laser beams was reported for the first time [19]. Liang et al. generated solar laser emissions through the end-side-pumping of three 3.0 mm diameter, 25 mm length Nd:YAG rods within a single conical pump cavity with a heliostat-parabolic system. The total multimode solar laser power of 18.3 W was measured from an effective collection area of 1.0 m^2, resulting in an 18.3 W/m^2 collection efficiency and 2.2% solar-to-laser conversion efficiency. Liang et al. also measured 16.5 W for the total multimode laser power by end-side-pumping three 2.5 mm diameter, 25 mm length Ce:Nd:YAG rods through a parabolic mirror with a 0.4 m^2 collection area, leading to the state-of-the-art multirod solar laser collection and solar-to-laser conversion efficiencies of 41.3 W/m^2 and 4.6%, respectively [20].

The multirod approach has the great advantage of solar tracking error compensation capacity [21]. Solar tracking systems (STS) are essential for maintaining the solar concentrator performance during the day and thus preserving the solar collection efficiency [22]. An accurate STS is important for orienting the solar collector and/or concentrator towards the sun in both altitude and azimuthal directions [23]. The tracking motion and angle of rotation change throughout the day. Depending on the location and date of the observation, an STS can have more frequent adjustments on the azimuthal direction around the solar noon than in the morning and afternoon, being more stable on the altitude angle [24]. Continuous tracking of the Sun can consume excessive energy and reduce the system efficiency and lifespan. A single-axis STS can attain a direct tracking error smaller than $\pm 0.40^\circ$,

whereas a more complex STS, that makes use of a dual-axis mechanism, can directly track the Sun with an error of ±0.15° [25,26]. Still, an STS with an error below 0.2° can cost about 10 times more than a similar system with double the solar tracking error [22]. The design of solar laser system needs to take this factor into account. It is economically advantageous to develop solar laser systems that can maintain their performance while using an STS with a relatively large tracking error. A dual-rod side-pumped solar laser has been experimentally investigated to tolerate a high tracking error and emit relatively stable laser beams, despite the limited collection and solar-to-laser conversion efficiencies of 14.1 W/m^2 and 1.8%, respectively. Solar tracking error widths at a 10% laser power loss ($TEW_{10\%}$) of 1.40° and 0.60° in the altitude and azimuthal directions, respectively, were attained [21]. Compared to side-pumping, end-side-pumping configurations achieve high efficiencies [12–15]. However, the solar energy is concentrated and focused onto the end face of the laser rod, which restricts the solar tracking error compensation capacity, especially in single-rod systems, because any slight tracking error in either the azimuthal or altitude axis causes a significant reduction in or even the extinction of the solar laser output [21]. Therefore, end-side-pumping a set of multiple closely coupled rods within a single pump cavity have been numerically analyzed with the aim of obtaining high efficiency while maintaining a high tracking error tolerance [27,28]. Catela et al. numerically studied a four-rod solar laser concept to obtain a high collection efficiency of 24.7 W/m^2 and solar-to-laser conversion efficiency of 2.6%, while attaining a 0.76° $TEW_{10\%}$ [27]. Further numerical improvement was achieved by Costa et al., using a seven-rod solar laser approach that allowed for a 0.99° $TEW_{10\%}$ and achieved a 23.3 W/m^2 collection efficiency and 2.5% solar-to-laser conversion efficiency [28]. Despite the high tracking error compensation capacity and efficiency by both solar laser systems, the laser power was not uniformly extracted from all the pumped laser rods, with some rods contributing more to the total laser power than others under the solar tracking error condition [27,28]. Uniform and stable emission from all rods is important for laser applications that make use of multiple laser beams, such as welding, brazing, surface texturing, laser ablation, drilling, and cutting [16–18].

A six-rod end-side-pumping approach for achieving uniform and stable emission from all rods in a solar laser system under non-continuous solar tracking is here proposed. Due to its significantly reduced weight and cost that make it a better choice for solar laser pumping in space as compared to other parabolic-type concentrators, a Fresnel lens was used to collect and concentrate solar rays towards a single solar laser head, where six Nd:YAG rods were simultaneously end-side-pumped. The laser head was composed of an aspherical lens, a light-guide homogenizer, and a conical pump cavity, and was compared to a similar laser head without the light guide. Numerical analysis was conducted to demonstrate that the solar laser head using the homogenizer could emit six 1064 nm laser beams with similar multimode powers under non-continuous tracking, hence achieving a uniform and stable emission from all rods.

2. Six-Rod Solar Laser System

2.1. Fresnel Lens

A Fresnel lens with a 1.5 m diameter (1.77 m^2 collection area), 0.93 m radius of curvature, and focal length of around 2.1 m was used as the primary concentrator (Figure 1). A Fresnel lens is typically made of polymethyl methacrylate, which has a high transmission efficiency for both visible and near-infrared wavelengths between 350 nm and 900 nm. A transmission efficiency of 78% was numerically calculated, considering the whole solar spectrum. Assuming a typical direct solar irradiance of 950 W/m^2 that is common in many Sun-rich countries around the world, 1312 W of solar power could be focused by the Fresnel lens. The proposed Fresnel lens can be installed onto a dual-axis STS.

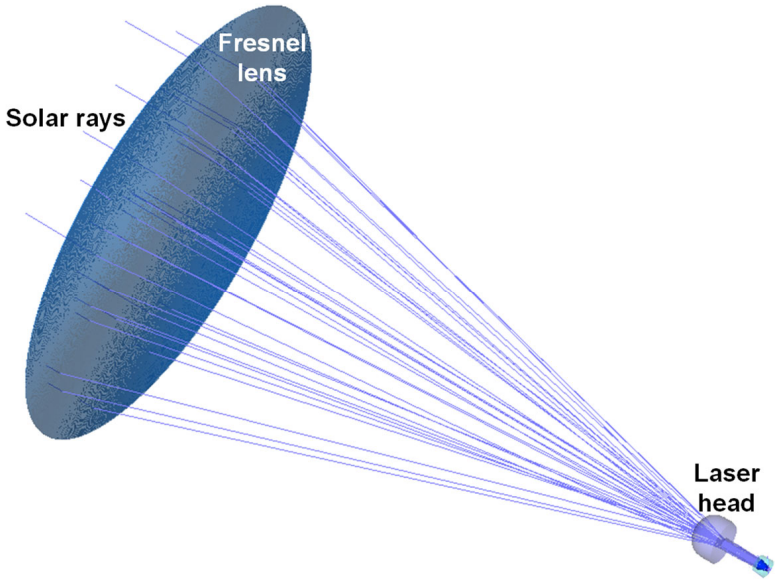

Figure 1. Design of the six-rod laser pumping system by a Fresnel lens.

2.2. Six-Rod Solar Laser Head

The solar laser head was composed of an aspherical lens, which coupled the concentrated solar radiation from the focal zone of the Fresnel lens into a hexagonal light guide, which transmitted and homogenized the radiation into a conical pump cavity within which the six Nd:YAG rods were evenly arranged (Figure 2).

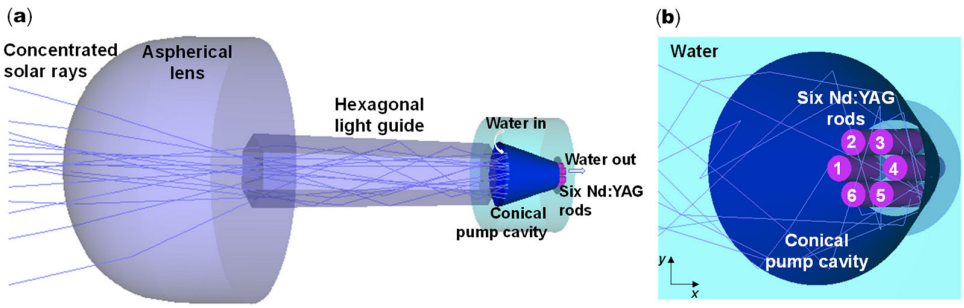

Figure 2. Design of the (**a**) six-rod laser head and (**b**) conical pump cavity with the six Nd:YAG rods (1–6).

The fused silica aspherical lens had a 140 mm diameter, 100 mm height, and −70 mm rear radius. The fused silica hexagonal light guide had a 34 mm input face width, 28 mm output face width, and 130 mm height. The hollow conical pump cavity with a 95% inner surface reflectivity had a 34 mm input aperture diameter, 14 mm output aperture diameter, and 31 mm height. Water was used as the cooling fluid, as shown in Figure 2.

3. Numerical Analysis of the Six-Rod Solar Laser System

Similar to previous solar laser studies [27,28], all the aforementioned design parameters of the six-rod solar laser system were first optimized by nonsequential ray-tracing Zemax® software to attain the maximum absorbed pump power and ensure power stability in each rod for typical azimuthal and altitude solar tracking errors up to ±0.5°. For the 1.0 at.% Nd:YAG laser medium, 22 peak absorption wavelengths from the standard solar spectrum for one-and-a-half air mass were defined in the Zemax® numerical data [29]. The direct solar irradiance of 950 W/m^2 was assumed. The effective pump power of the light source considered the 16% overlap between the Nd:YAG absorption spectrum and the solar spectrum [30]. Spectral variation such as transmission through the Fresnel lens and the reflectance of the conical pump cavity were introduced. The absorption spectra

of fused silica and water were included in the glass catalogue data of Zemax® [14]. In the ray-tracing analysis, a detector volume divided into 24,000 voxels was used for each rod, and the path length of the rays through each voxel was found. With these values and the effective absorption coefficient of 1.0 at.% Nd:YAG material, the total absorbed pump power was numerically calculated by summing up the absorbed pump radiation of all voxels.

The absorbed power data from the Zemax® analysis were then imported into the LASCAD™ software to calculate the multimode solar laser power, optimizing the laser resonator parameters. A fluorescence lifetime of 230 μs, a stimulated emission cross section of 2.8×10^{-19} cm^2 [31], an averaged solar pump wavelength of 660 nm [10], and a typical absorption and scattering loss of 0.002 cm^{-1} [20] for the 1.0 at.% Nd:YAG medium were adopted in the LASCAD™ analysis.

Each of the six optical resonators in the LASCAD™ software was comprised of two opposing parallel mirrors: the high reflection (HR 1064 nm, 99.98%) coating on the upper end face of the Nd:YAG rod, and the partial reflection (PR 1064 nm) coated output mirror, with reflectivity varying between 90% and 99%. L represents the separation length between the antireflection (AR 1064 nm) coating on the lower end face of each rod and the respective PR1064 nm output mirror (Figure 3). A plane-concave optical resonator with a small L was employed, ensuring that the energy of higher-order modes was not wasted by diffraction losses.

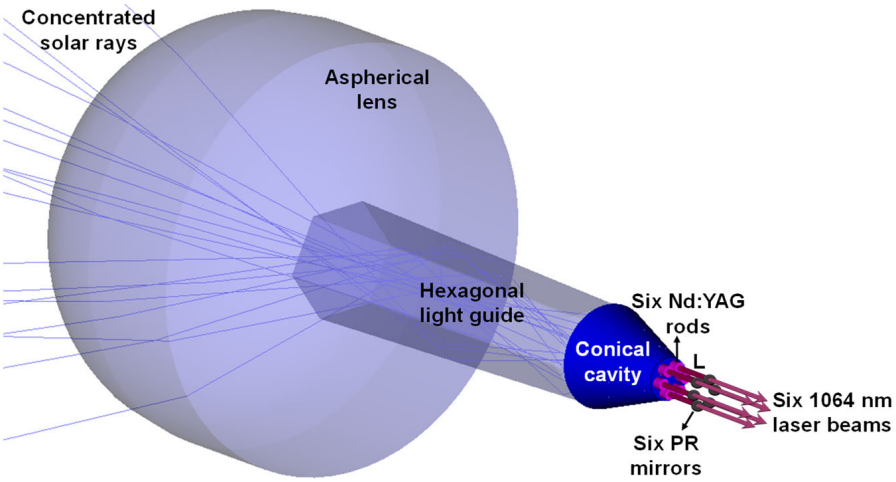

Figure 3. Schematic representation of the solar laser head with the laser resonant cavity. L represents the separation length between the lower end face of the Nd:YAG rod and the partial reflection (PR) output mirror.

4. Six-Rod Solar Laser Performance

The performance of the six-rod solar laser head was optimized and analyzed by both Zemax® and LASCAD™ software. Besides the laser head with the aspherical lens and hexagonal light guide, another laser head with only the aspherical lens as part of the second stage was also studied to compare the performance of the laser with and without the light-guide homogenizer. In Figure 4, the absorbed pump flux distributions along the longitudinal and five transversal cross sections of one of the six 1.0 at.% Nd:YAG laser rods from both laser heads is shown. Only one rod is presented because all rods in each laser head had similar absorbed pump flux distributions. The rod from the laser head with the light guide demonstrated a more symmetric and uniform absorbed pump profile than that from the laser head with no light guide (Figure 4), proving that the homogenizer helps to evenly distribute the pump power among the laser rods.

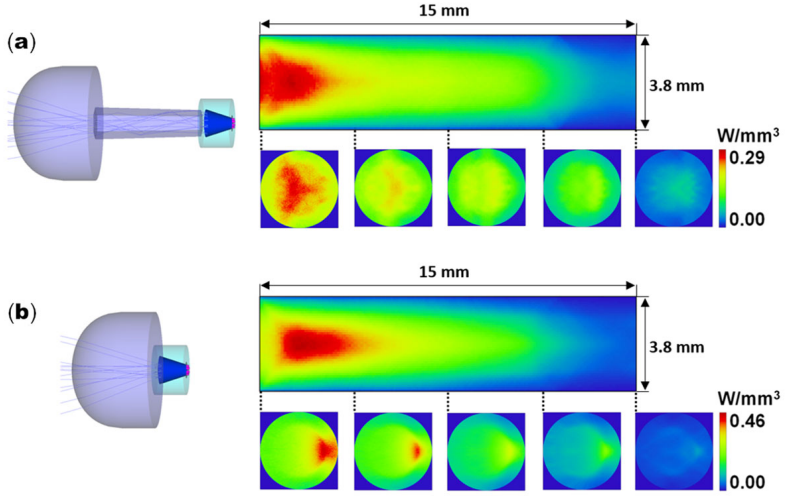

Figure 4. Absorbed pump flux distributions along the longitudinal and five transversal cross sections of a 3.8 mm diameter, 15 mm length Nd:YAG rod in the laser head with: (**a**) the aspherical lens and hexagonal light guide, and (**b**) only the aspherical lens.

The Nd:YAG rod diameter was optimized for the laser head with the aspherical lens and light guide. In Figure 5, the total multimode laser power from the six rods as a function of the solar tracking error in the azimuthal direction, for different rod diameters, is represented. The laser head with 3.8 mm diameter, 15 mm length Nd:YAG rods presented not only the maximum total laser power of 34.0 W, but also the best $TEW_{10\%}$ of 0.72°.

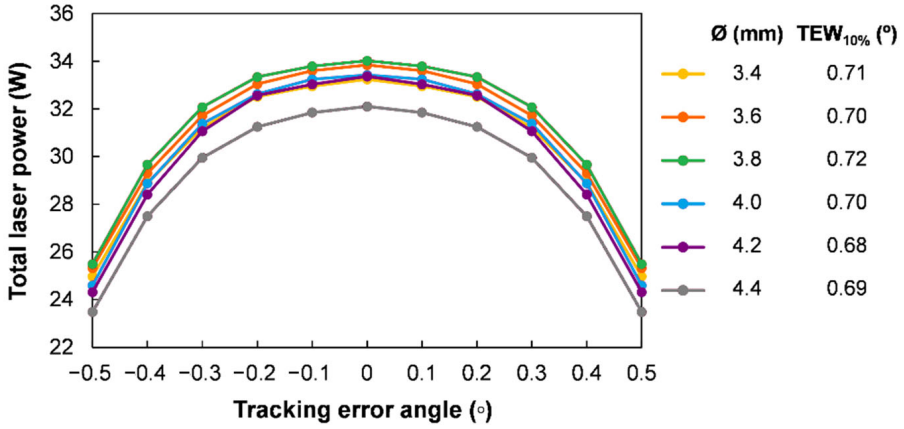

Figure 5. Total multimode solar laser power as a function of the azimuthal solar tracking error for different laser rod diameters (Ø), using the laser head with the aspherical lens and light guide. The tracking error width at 10% loss total multimode solar laser power ($TEW_{10\%}$) is also indicated.

The best rod dimension, 3.8 mm diameter with 15 mm length, was then used for the laser head without the light guide. The total multimode laser power from both laser heads was compared by studying it as a function of the solar tracking error in the azimuthal ($\Delta\alpha$) and altitude (Δh) directions, as shown in Figure 6. Each solar laser head evidenced a symmetric tracking error compensation capacity for the azimuthal and altitude directions, having a similar total laser power and $TEW_{10\%}$ in both directions. The laser head without the light guide had a higher maximum total laser power of 39.6 W, but a lower $TEW_{10\%}$ of 0.69°, than the one with the light guide (Figure 6). Therefore, both laser heads could operate with a more simple and less expensive STS [22].

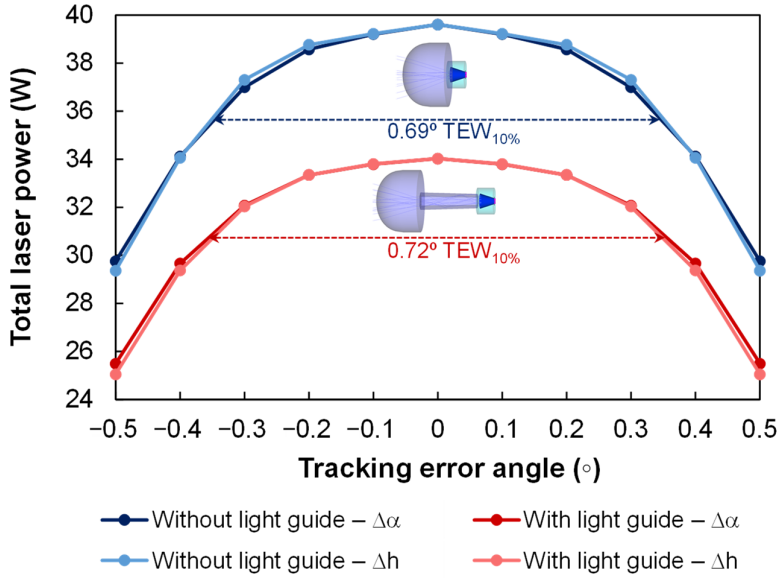

Figure 6. Total multimode solar laser power, from the six rods with 3.8 mm diameter and 15 mm length, as a function of the solar tracking error in the azimuthal (Δα) and altitude (Δh) directions, for the laser head with the aspherical lens and light guide, and the laser head with only the aspherical lens. The tracking error width at 10% loss total multimode solar laser power ($TEW_{10\%}$) is also indicated.

Even though the light guide in the laser head led to a slightly improved solar tracking error compensation capacity, the most pronounced effects relied on the uniform absorbed pump power and laser emission by the six rods. The absorbed pump flux distributions and the individual laser power from the six rods of each of the two laser heads were analyzed as a function of the azimuthal and altitude solar tracking errors to explore their uniformity performance, as shown in Figures 7 and 8. The absorbed pump profiles of the six rods in the laser head with the light guide were more uniform along the solar tracking error angles in both the azimuthal and altitude directions than that in the laser head without the light guide. The laser power was also more uniform with much less variation between the rods for the laser head with light guide. For example, under the extreme tracking error condition of $\Delta\alpha = \Delta h = 0.5^\circ$, the laser power from the six rods only varied from 1.70 W to 2.22 W using the light guide, in contrast to the large variation from 0.80 W to 4.50 W without it. The light guide demonstrated the ability to homogenize the pump power absorbed by all rods under solar tracking error variation, being essential in the production of uniform laser power emission by all rods of the multirod scheme.

The laser emission uniformity performance is also demonstrated in Figure 9. The laser head with the light guide produced six solar laser emissions with almost the same laser power, even under the most extreme solar tracking error condition of $\pm 0.5^\circ$ (Figure 9a). On the contrary, the laser head without the light guide produced six laser emissions with significantly different laser powers under solar tracking error variation (Figure 9b).

To better analyze the variation in the laser power among the six rods, the coefficient of variation (CV) was studied as a function of the azimuthal solar tracking error, for both laser heads (Figures 10 and 11). The CV of the laser power extracted from the six rods in the laser head with the light guide was investigated for the several rod diameters (Figure 10). All diameters revealed low CVs under the solar tracking error condition. However, the 3.8 mm and the 4.0 mm rod diameters presented the best performances. Using the 3.8 mm diameter Nd:YAG rods, the CV slowly increased to only 2.17% at a $\pm 0.5^\circ$ tracking error angle. The CV of the 4.0 mm diameter, 15 mm length Nd:YAG rods also had a similar behavior, reaching only 1.78% at the tracking error angle of $\pm 0.5^\circ$ (Figure 10).

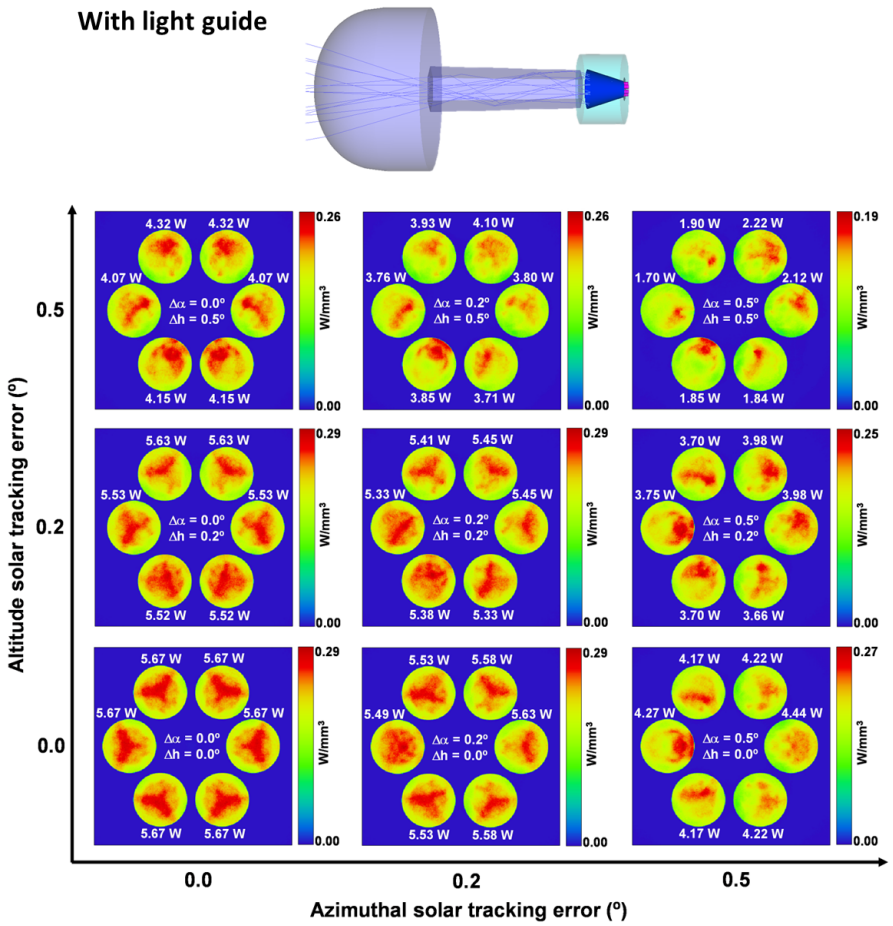

Figure 7. Absorbed pump flux distributions along the top cross section of the six rods with 3.8 mm diameter, 15 mm length, in the laser head with the aspherical lens and light guide, as a function of the solar tracking error in the azimuthal (Δα) and altitude (Δh) directions. The multimode solar laser power emitted by each rod is also indicated.

In Figure 11, the CVs of the 3.8 mm diameter, 15 mm length rods in both laser heads with and without the light guide are shown, as well as the CV results from the previous work with seven 4.0 mm diameter, 13 mm length Nd:YAG rods in a laser head with an aspherical lens and a conical pump cavity [28]. The CV of the laser head with the light guide was much lower under the solar tracking error condition than that of the other laser heads without light guide (Figure 11). For the laser head with no light guide, a maximum CV of 52.31% was achieved at the tracking error angle of ±0.5°. A maximum CV of 165.63% was obtained from the laser head of the previous work at the same tracking error angle (Figure 11) [28]. The homogenizer was thus essential to reduce the CV and maintain the uniformity of the laser power emission among the rods under the solar tracking error condition.

Overall, even though the six-rod laser approach without the homogenizer produced a greater laser power of 39.6 W corresponding to a 22.4 W/m^2 collection efficiency and 2.4% solar-to-laser power conversion efficiency, the $TEW_{10\%}$ of 0.69° and the high CV of the laser power among the rods of 52.31% at the tracking error angle of ±0.5° were worse than the ones obtained by the six-rod laser with the homogenizer. This approach with the light guide produced a 34.0 W laser power, corresponding to a 19.2 W/m^2 collection efficiency and 2.0% solar-to-laser power conversion efficiency, but achieved a $TEW_{10\%}$ of 0.72° and a remarkable CV of only 2.17% at the tracking error angle of ±0.5° that was 4.2 times better than that without the light guide. These results demonstrate the great utility of the homogenizer to help in extracting a stable and similar laser power from all the laser rods even under solar tracking error variation.

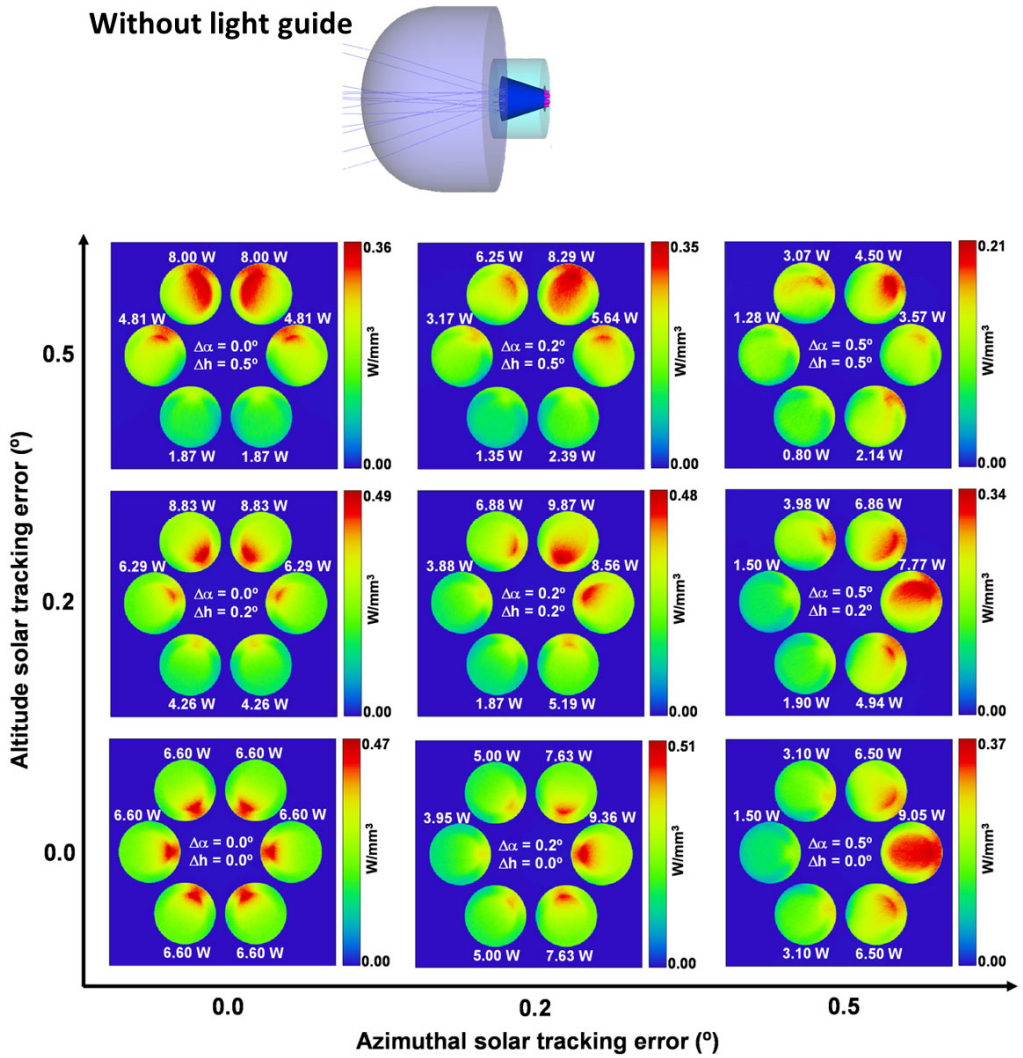

Figure 8. Absorbed pump flux distributions along the top cross section of the six rods with 3.8 mm diameter, 15 mm length, in the laser head with only the aspherical lens, as a function of the solar tracking error in the azimuthal ($\Delta\alpha$) and altitude (Δh) directions. The multimode solar laser power numerically calculated for each rod is also indicated.

Comparing this work with the previous numerical work of Costa et al. who used a seven-rod laser head without a homogenizer [28], the 23.3 W/m^2 collection efficiency, 2.5% solar-to-laser conversion efficiency, and 0.99° TEW$_{10\%}$ were higher than the ones obtained with the present solar laser head with homogenizer. However, the CV of the laser power among the rods was very high, 165.63% at the tracking error angle of $\pm$0.5°, which is 76 times more than the CV from the six-rod laser head using the light guide. This makes the proposed solar laser approach with homogenizer ideal for multibeam laser applications where stability and uniformity of the laser power are indispensable.

Recent advances in the concentrator design have shown promise in achieving higher concentration ratios and more efficient light collection [32–34]. The future inclusion of these novel solar concentrators may further help to boost solar laser efficiency. More importantly, Ce:Nd:YAG solar laser systems have also shown higher absorption efficiency in previous studies when compared to Nd:YAG, leading to higher efficiencies [20].

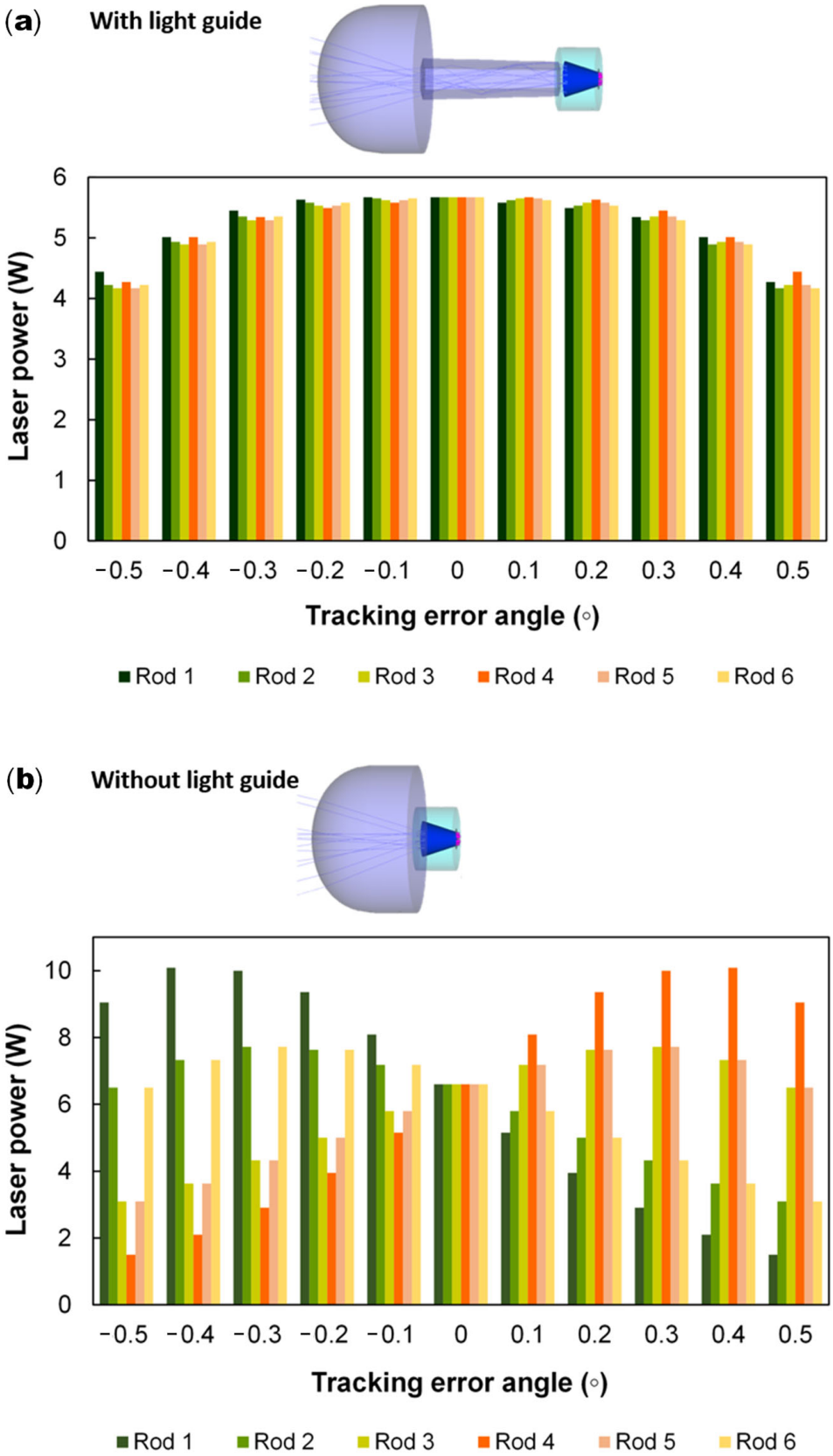

Figure 9. Multimode solar laser power obtained from each of the six 3.8 mm diameter, 15 mm length Nd:YAG rods as a function of the azimuthal solar tracking error, using (**a**) the laser head with the aspherical lens and light guide, and (**b**) the laser head with only the aspherical lens, without the light guide.

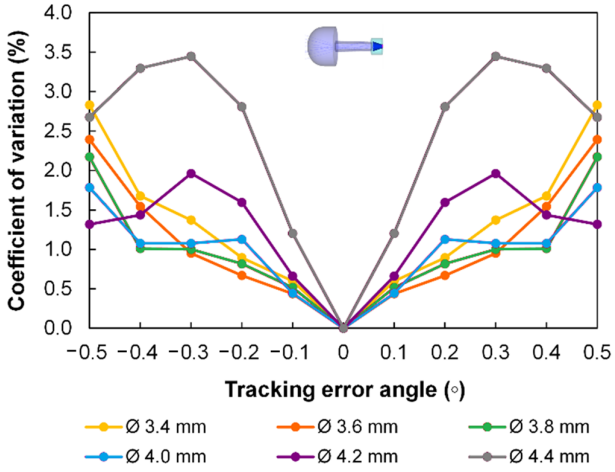

Figure 10. Coefficient of variation of the multimode solar laser power obtained from the six Nd:YAG rods as a function of the azimuthal solar tracking error for the laser head with the light guide, for different laser rod diameters (Ø).

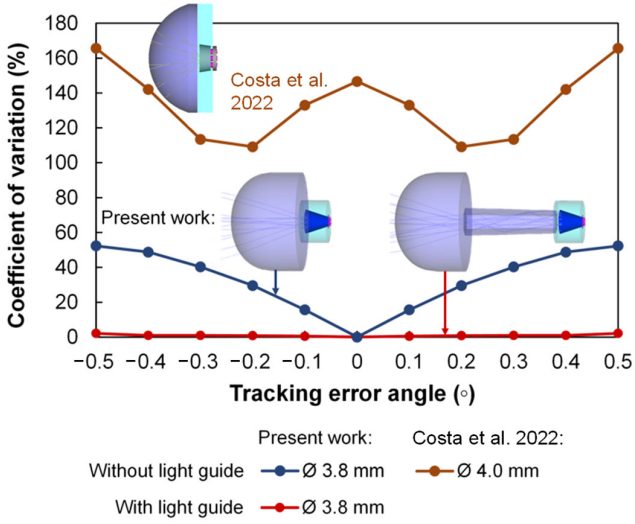

Figure 11. Coefficient of variation of the multimode solar laser power obtained from the Nd:YAG rods as a function of the azimuthal solar tracking error for both six-rod laser heads, with and without the light guide, using the 3.8 mm diameter (Ø), 15 mm length rods, and the seven-rod scheme using the 4.0 mm diameter, 13 mm length rods from Costa et al., 2022 [28].

5. Conclusions

A six-rod solar laser approach was proposed here to enable uniform and stable laser power emitted by the rods under non-continuous solar tracking. A Fresnel lens was used as the primary concentrator. The laser head was composed of a second-stage aspherical lens/light-guide homogenizer and a third-stage conical pump cavity with six Nd:YAG laser rods. Through numerical analysis, the laser scheme parameters were optimized to obtain the uniform and stable emission of six laser beams with similar multimode powers under solar tracking error variation. The laser performance from the solar head with only the aspherical lens as the second stage was also studied to better assess the advantage of the light guide on the laser performance. The efficiency of the laser head without the light guide was higher: 22.4 W/m^2 for the collection efficiency and 2.4% for the solar-to-laser power conversion efficiency; however, the $TEW_{10\%}$ of 0.69° and the CV of the laser power among the rods under non-continuous solar tracking, 52.31% at the tracking error angle of ±0.5°, were worse than the ones obtained by the six-rod laser head with the homogenizer. Even though this scheme resulted in lower collection and solar-to-laser power conversion

efficiencies of 19.2 W/m^2 and 2.0%, respectively, a higher TEW$_{10\%}$ of 0.72° and a remarkable CV of only 2.17% at the tracking error angle of ±0.5° were obtained. The CV value was also 76 times better than that of the previous numerical work. All this proves that the homogenizer is necessary to ensure similar multimode solar laser power extraction from all laser rods even under solar tracking error variation, which is essential for multibeam laser applications where power stability and uniformity are important.

Author Contributions: Conceptualization, C.R.V. and D.L.; methodology, C.R.V., D.L. and J.A.; software, C.R.V., J.A., H.C. and M.C.; validation, C.R.V., D.L., J.A. and M.C.; formal analysis, C.R.V., D.L. and J.A.; investigation, C.R.V., D.L., J.A., M.C., H.C., D.G. and B.D.T.; resources, D.L. and J.A.; data curation, C.R.V., D.G. and B.D.T.; writing—original draft preparation, C.R.V. and D.L.; writing—review and editing, C.R.V., D.L., J.A., M.C., H.C., D.G. and B.D.T.; supervision, D.L.; project administration, D.L.; funding acquisition, D.L. and J.A. All authors have read and agreed to the published version of the manuscript.

Funding: This research was funded by the Science and Technology Foundation of Portuguese Ministry of Science, Technology and Higher Education (FCT-MCTES), through the strategic project UIDB/00068/2020 and the exploratory research project EXPL/FIS-OTI/0332/2021.

Institutional Review Board Statement: Not applicable.

Informed Consent Statement: Not applicable.

Data Availability Statement: Not applicable.

Acknowledgments: The FCT-MCTES fellowship grants SFRH/BPD/125116/2016, SFRH/BD/145322/2019, 2021.06172.BD, PD/BD/1428/2018, and CEECIND/03081/2017 of Cláudia R. Vistas, Miguel Catela, Hugo Costa, Dário Garcia and Joana Almeida, respectively, are acknowledged.

Conflicts of Interest: The authors declare no conflict of interest.

References

1. Kiss, Z.J.; Lewis, H.R.; Duncan, R.C. Sun pumped continuous optical maser. *Appl. Phys. Lett.* **1963**, *2*, 93–94. [CrossRef]
2. Young, C.G. A Sun-Pumped CW One-Watt Laser. *Appl. Opt.* **1966**, *5*, 993–997. [CrossRef] [PubMed]
3. Yabe, T.; Bagheri, B.; Ohkubo, T. 100 W-class solar pumped laser for sustainable magnesium-hydrogen energy cycle. *J. Appl. Phys.* **2008**, *104*, 83104. [CrossRef]
4. Lando, M.; Kagan, J.A.; Shimony, Y.; Kalisky, Y.Y.; Noter, Y.; Yogev, A.; Rotman, S.R.; Rosenwaks, S. Solar-pumped solid state laser program. In Proceedings of the 10th Meeting on Optical Engineering in Israel, Jerusalem, Israel, 1–6 March 1997; Volume 3110, p. 196. [CrossRef]
5. Vasile, M.; Maddock, C.A. Design of a formation of solar pumped lasers for asteroid deflection. *Adv. Space Res.* **2012**, *50*, 891–905. [CrossRef]
6. Yamada, N.; Ito, T.; Ito, H.; Motohiro, T.; Takeda, Y. Crystalline silicon photovoltaic cells used for power transmission from solar-pumped lasers: III. Prototype for proof of the light trapping concept. *Jpn. J. Appl. Phys.* **2018**, *57*, 08RF07. [CrossRef]
7. Fernández, E.F.; García-Loureiro, A.; Seoane, N.; Almonacid, F. Band-gap material selection for remote high-power laser transmission. *Sol. Energy Mater. Sol. Cells* **2022**, *235*, 111483. [CrossRef]
8. Lousteau, J.; Negro, D.; Mura, E.; Scarpignato, G.C.; Perrone, G.; Abrate, S.; Boetti, N.G.; Milanese, D. Solar pumping of solid state lasers for space mission: A novel approach. *SPIE* **2017**, *10564*, 1056418. [CrossRef]
9. Arashi, H.; Oka, Y.; Sasahara, N.; Kaimai, A.; Ishigame, M. A Solar-Pumped CW 18 W Nd:YAG Laser. *Jpn. J. Appl. Phys.* **1984**, *23*, 1051–1053. [CrossRef]
10. Weksler, M.; Shwartz, J. Solar-pumped solid-state lasers. *IEEE J. Quantum Electron.* **1988**, *24*, 1222–1228. [CrossRef]
11. Dinh, T.H.; Ohkubo, T.; Yabe, T.; Kuboyama, H. 120 watt continuous wave solar-pumped laser with a liquid light-guide lens and an Nd:YAG rod. *Opt. Lett.* **2012**, *37*, 2670–2672. [CrossRef]
12. Liang, D.; Almeida, J.; Vistas, C.R.; Guillot, E. Solar-pumped Nd:YAG laser with 31.5 W/m^2 multimode and 7.9 W/m^2 TEM$_{00}$-mode collection efficiencies. *Sol. Energy Mater. Sol. Cells* **2017**, *159*, 435–439. [CrossRef]
13. Liang, D.; Vistas, C.R.; Tibúrcio, B.D.; Almeida, J. Solar-pumped Cr:Nd:YAG ceramic laser with 6.7% slope efficiency. *Sol. Energy Mater. Sol. Cells* **2018**, *185*, 75–79. [CrossRef]
14. Garcia, D.; Liang, D.; Vistas, C.R.; Costa, H.; Catela, M.; Tibúrcio, B.D.; Almeida, J. Ce:Nd:YAG Solar Laser with 4.5% Solar-to-Laser Conversion Efficiency. *Energies* **2022**, *15*, 5292. [CrossRef]
15. Cai, Z.; Zhao, C.; Zhao, Z.; Zhang, J.; Zhang, Z.; Zhang, H. Efficient 38.8 W/m^2 solar pumped laser with a Ce:Nd:YAG crystal and a Fresnel lens. *Opt. Express* **2023**, *31*, 1340–1353. [CrossRef]

16. Strite, T.; Gusenko, A.; Grupp, M.; Hoult, T. Fiber Lasers: Multiple Laser Beam Materials Processing. Available online: https://www.laserfocusworld.com/lasers-sources/article/16547084/fiber-lasers-multiple-laser-beam-materials-processing (accessed on 2 August 2022).
17. Gillner, A.; Finger, J.; Gretzki, P.; Niessen, M.; Bartels, T.; Reininghaus, M. High power laser processing with ultrafast and multi-parallel beams. *J. Laser Micro Nanoeng.* **2019**, *14*, 129–137. [CrossRef]
18. Olsen, F.O.; Hansen, K.S.; Nielsen, J.S. Multibeam fiber laser cutting. *J. Laser Appl.* **2009**, *21*, 133–138. [CrossRef]
19. Liang, D.; Almeida, J.; Garcia, D.; Tibúrcio, B.D.; Guillot, E.; Vistas, C.R. Simultaneous solar laser emissions from three Nd:YAG rods within a single pump cavity. *Sol. Energy* **2020**, *199*, 192–197. [CrossRef]
20. Liang, D.; Vistas, C.R.; Garcia, D.; Tibúrcio, B.D.; Catela, M.; Costa, H.; Guillot, E.; Almeida, J. Most efficient simultaneous solar laser emissions from three Ce:Nd:YAG rods within a single pump cavity. *Sol. Energy Mater. Sol. Cells* **2022**, *246*, 111921. [CrossRef]
21. Tibúrcio, B.D.; Liang, D.; Almeida, J.; Garcia, D.; Catela, M.; Costa, H.; Vistas, C.R. Tracking error compensation capacity measurement of a dual-rod side-pumping solar laser. *Renew. Energy* **2022**, *195*, 1253–1261. [CrossRef]
22. Angulo-Calderón, M.; Salgado-Tránsito, I.; Trejo-Zúñiga, I.; Paredes-Orta, C.; Kesthkar, S.; Díaz-Ponce, A. Development and Accuracy Assessment of a High-Precision Dual-Axis Pre-Commercial Solar Tracker for Concentrating Photovoltaic Modules. *Appl. Sci.* **2022**, *12*, 2625. [CrossRef]
23. Kalogirou, S.A. *Solar Energy Engineering: Processes and Systems*, 2nd ed.; Academic Press: Cambridge, MA, USA, 2014; ISBN 9780123972705.
24. Jin, X.; Xu, G.; Zhou, R.; Luo, X.; Quan, Y. A Sun Tracking System Design for a Large Dish Solar Concentrator. *Int. J. Clean Coal Energy* **2013**, *2*, 16–20. [CrossRef]
25. Sallaberry, F.; Pujol-Nadal, R.; Larcher, M.; Rittmann-Frank, M.H. Direct tracking error characterization on a single-axis solar tracker. *Energy Convers. Manag.* **2015**, *105*, 1281–1290. [CrossRef]
26. Yao, Y.; Hu, Y.; Gao, S.; Yang, G.; Du, J. A multipurpose dual-axis solar tracker with two tracking strategies. *Renew. Energy* **2014**, *72*, 88–98. [CrossRef]
27. Catela, M.; Liang, D.; Vistas, C.R.; Garcia, D.; Costa, H.; Tibúrcio, B.D.; Almeida, J. Highly Efficient Four-Rod Pumping Approach for the Most Stable Solar Laser Emission. *Micromachines* **2022**, *13*, 1670. [CrossRef]
28. Costa, H.; Liang, D.; Almeida, J.; Catela, M.; Garcia, D.; Tibúrcio, B.D.; Vistas, C.R. Seven-Rod Pumping Concept for Highly Stable Solar Laser Emission. *Energies* **2022**, *15*, 9140. [CrossRef]
29. *ASTM G173-03(2012)*; Standard Tables for Reference Solar Spectral Irradiances: Direct Normal and Hemispherical on 37° Tilted Surface. ASTM International: West Conshohocken, PA, USA, 2012.
30. Zhao, B.; Zhao, C.; He, J.; Yang, S. The study of active medium for solar-pumped solid-state lasers. *Acta Opt. Sin* **2007**, *27*, 1797–1801.
31. Koechner, W. *Solid-State Laser Engineering*, 6th ed.; Springer Series in Optical Sciences; Springer: New York, NY, USA, 2006; ISBN 978-0-387-29338-7.
32. Almonacid, F.; Fernández, E.F.; Pérez-Higueras, P.; Ferrer-Rodríguez, J.P. Optical design of a 4-off-axis-unit Cassegrain ultra-high concentrator photovoltaics module with a central receiver. *Opt. Lett.* **2016**, *41*, 1985–1988. [CrossRef]
33. Ferrer-Rodríguez, J.P.; Saura, J.M.; Fernández, E.F.; Almonacid, F.; Talavera, D.L.; Pérez-Higueras, P. Exploring ultra-high concentrator photovoltaic Cassegrain-Koehler-based designs up to 6000×. *Opt. Express* **2020**, *28*, 6609–6617. [CrossRef]
34. Baig, H.; Siviter, J.; Li, W.; Paul, M.C.; Montecucco, A.; Rolley, M.H.; Sweet, T.K.N.; Gao, M.; Mullen, P.A.; Fernandez, E.F.; et al. Conceptual design and performance evaluation of a hybrid concentrating photovoltaic system in preparation for energy. *Energy* **2018**, *147*, 547–560. [CrossRef]